Journal of Membrane Science 668 (2023) 121184

Contents lists available at ScienceDirect

Journal of Membrane Science

journal homepage: www.elsevier.com/locate/memsci

Influence of electrolyte on concentration-induced conductivity-permselectivity tradeoff of ion-exchange membranes

Yuxuan Huang [a], Hanqing Fan [a], Ngai Yin Yip [a,b,*]

[a] Department of Earth and Environmental Engineering, Columbia University, NY, 10027-6623, United States
[b] Columbia Water Center, Columbia University, NY, 10027-6623, United States

ARTICLE INFO

Keywords:
Ion-exchange membranes
Conductivity-permselectivity tradeoff
Ion valency
Ion mobility
Donnan exclusion

ABSTRACT

In ion-exchange membranes (IEMs), the concentration-induced tradeoff between conductivity and permselectivity constrains process performance. This study investigates the impacts of different electrolytes on the conductivity-permselectivity tradeoff of commercial cation and anion exchange membranes. Nine different electrolyte solutions containing mono-, di-, and trivalent ions, and spanning 1.5 orders of magnitude in concentration were examined. Effective conductivity is found to be determined by valency and mobility of the counterion and is insensitive to the co-ion identity. Apparent permselectivity declines with higher valency of the counterion and with lower valency of the co-ion. Overall, the IEMs exhibited different conductivity-permselectivity tradeoff behaviors across the electrolyte solutions investigated. The disparate tradeoff trends are shown to be governed by counter- and co-ion valencies, and counterion diffusivity. The study sheds light on the principal factors underpinning the tradeoff and advances the understanding of attainable conductivity-permselectivity performance in more complex water chemistries that are pertinent for practical IEM applications.

1. Introduction

Ion-exchange membranes (IEMs) are polymeric films with a high density of charged functional groups, which allow the selective transport of oppositely-charged counterions, while retaining like-charged co-ions by charge exclusion [1–3]. Membranes with negative fixed charges, e.g., sulfonate, preferentially allow the transport of cations and are classified as cation exchange membranes (CEMs), whereas anion exchange membranes (AEMs) have positive fixed charges, e.g., quaternary amines, and selectively permeate anions [1,4]. IEMs have been broadly employed in water, energy, and chemical production applications, such as electrodialysis desalination, redox flow batteries, and the chlorine-alkaline process, respectively [5–7]. The performance of IEM-based technologies is largely determined by the two principal parameters of ionic conductivity and permselectivity [1,4]. Ionic conductivity determines contribution of the IEMs to overall stack resistance and, thus, affects energy consumption and process kinetics or, equivalently, membrane area required. Permselectivity quantifies the membrane selectivity for counterion transport over co-ion and, hence, influences current efficiency and separation specificity. Both high conductivity and high permselectivity are desired in almost all IEM applications.

Permselectivity and ionic conductivity are not intrinsic properties of the membranes but are affected by operating conditions, specifically composition and concentration of the external solutions. Recent studies revealed a tradeoff relationship between IEM conductivity and permselectivity induced by solution concentration: an increase in concentration of the external NaCl solution enhances conductivity but compromises permselectivity between Na^+ and Cl^- [8–10]. The conductivity-permselectivity tradeoff constrains the performance of IEM processes and can also narrow the scope of application [8]. IEMs operate in different electrolytes beyond pure NaCl solutions [3,11,12]. Therefore, it is of significance to study the tradeoff behaviors of IEMs in various electrolytes and shed light on the underlying factors governing the tradeoffs. Previous work characterized the conductivity, or resistance, of IEMs in a range of electrolytes and concentrations [9,13,14], and other studies evaluated membrane permselectivity in electrolytes besides NaCl [11,15,16]. However, these investigations focused separately on either conductivity or permselectivity; comprehensive and systematic studies that simultaneously examine IEM conductivity, permselectivity, and the tradeoff relationship in different electrolyte solutions and concentrations are absent.

* Corresponding author. Department of Earth and Environmental Engineering, Columbia University, NY, 10027-6623, United States.
E-mail address: n.y.yip@columbia.edu (N.Y. Yip).

https://doi.org/10.1016/j.memsci.2022.121184
Received 17 August 2022; Received in revised form 23 October 2022; Accepted 11 November 2022
Available online 17 November 2022

This study investigates the influence of electrolyte on the concentration-induced conductivity-permselectivity tradeoff of cation and anion exchange membranes. Effective ionic conductivities and apparent permselectivities of commercial IEMs were characterized in nine different electrolyte solutions containing mono-, di-, and trivalent ions, over four concentrations spanning 1.5 orders of magnitude. Effects of counter- and co-ion identities on the conductivities and permselectivities were analyzed to elucidate the principal factors and governing mechanisms underpinning the observed trends. The analysis then examines the role of electrolyte and solution concentration on the conductivity-permselectivity tradeoff. Lastly, implications for practical applications of IEM in different water chemistries are discussed.

2. Materials and methods

2.1. Membranes and chemicals

Commercial cation exchange membrane and anion exchange membrane, Selemion CMV and Selemion AMV, respectively, used in the study were acquired from Asahi Glass Co. (Japan). Ion exchange capacities of CMV and AMV are reported as 2.11 ± 0.02 and 1.95 ± 0.07 meq/g dry polymer, respectively, while swelling degrees in pure water are 0.314 ± 0.007 g water/g dry polymer for CMV (in Na^+ counterion) and 0.183 ± 0.003 g water/g dry polymer for AMV (in Cl^- counterion) [17]. The electrolytes investigated are NaCl, KCl, NH_4Cl, $MgCl_2$, $CaCl_2$, $AlCl_3$, NaBr, Na_2SO_4, and $MgSO_4$. All the salts are reagent grade and were purchased from Thermo Fisher Scientific (Waltham, MA). Deionized (DI) water was purified with a Milli-Q system (MilliporeSigma, Burlington, MA). Before conductivity or permselectivity measurements, membrane samples were equilibrated in 1.0 eq/L of the test solution for at least 24 h, to swap the counter- and co-ions in the membrane to the cation and anion being characterized.

2.2. Membrane characterization

2.2.1. Resistance and conductivity

Area specific resistances (ASRs) in the different electrolyte solutions at concentrations, c, of 0.030, 0.10, 0.30, and 1.0 eq/L were characterized using an electrochemical test setup based on a two-chamber cell system with a four-electrode configuration [1]. Membrane coupons were clamped between the two chambers of the cell, with an active membrane area of 3.14 cm^2 (2.0 cm diameter circle). Electrolyte solution volume in each chamber is ≈16 mL. On each end of the cell, one Pt-coated Ti mesh (4 cm × 4 cm) was used as working or counter electrodes. Two Ag/AgCl reference electrodes (BASi RE-5B, Bioanalytical Systems, Inc., West Lafayette, IN) were positioned 3.5 mm from either side of the membrane to measure the potential difference. Prior to resistance measurements, membrane samples were equilibrated in test solutions for 24 h, with the solution renewed after 12 h.

Direct current method was employed to characterize resistances since IEM applications are operated with unidirectional ion flow. The differences between direct and alternating current techniques can be found in literature [1,18,19]. An electrochemical workstation (Interface 1010E, Gamry Instruments, Warminster, PA) was used to measure the membrane resistance. Test solutions were circulated through both chambers of the test cell at 4 mL/min using a peristaltic pump (BT101S, Golander Pump, Norcross, GA). Direct current was applied to the system in galvanostatic mode from 1.0 to 10 mA (i.e., current density, i, of 0.32–3.2 mA/cm^2), in increments of 1.0 mA, and the potential difference between the two reference electrodes was recorded. At the lowest concentration of 0.030 eq/L, a smaller current range was used (0.10–1.0 mA, in increments of 0.10 mA). Each current step was maintained for 10 s and the voltage drop, V_m, was recorded every second. The slope of voltage drop as a function of current density, i.e., dV_m/di, gives the combined area resistance of the IEM and solution. Solution resistances were measured using the same protocol but without the IEM in the cell (dV_{blank}/di). Subtracting the blank reading from the combined resistance yields the ASR [20]:

$$\mathrm{ASR} = \frac{dV_m}{di} - \frac{dV_{blank}}{di} \tag{1}$$

Note that for NH_4Cl and $AlCl_3$, the cations, NH_4^+ and Al^{3+}, can deprotonate and complex with OH^-, respectively. Nonetheless, the predominant species in the corresponding solutions are NH_4^+ and Al^{3+} across the concentration range according to the acid dissociation and stability constants, and the concentration of H^+ was negligible relative to the cations.

Thicknesses of hydrated membrane coupons, l, were measured using a digital micrometer (Series 293, Mitutoyo Co., Japan). The effective ionic conductivity, κ, is then calculated using [9,20].

$$\kappa = \frac{l}{\mathrm{ASR}} \tag{2}$$

κ is termed effective ionic conductivity since it includes the contributions from the IEM and diffusion boundary layers (further elaborated in Section 3.1.1). For each electrolyte solution and concentration, at least three ASR measurements were carried out on the same membrane coupon.

2.2.2. Apparent permselectivity

Permselectivity is a measure of the ability of the IEM to selectively allow for counterion transport over co-ions. The static method was employed for this study to determine the apparent permselectivities. In the static characterization method, there is no net ionic flux across the membrane. Therefore, the measured permselectivity is slightly different from the true permselectivity in dynamic processes with net ionic fluxes, e.g., electrodialysis, and is, hence, termed the apparent permselectivity (discussions on the distinctions can be found in literature [1,12,21]). Nevertheless, apparent permselectivity has been found to adequately describe the ability of IEMs to differentiate between counter- and co-ions; the parameter is, thus, broadly adopted in IEM research [1,22,23]. Importantly, the analyses in this study focus on the trends in permselectivity with varying solution concentration and different counter- and co-ion identities; such trends are expected to hold for both true and apparent permselectivities. Two solutions of different concentrations contact the membrane on either side and the potential difference across the IEM was used to determine the apparent permselectivity, α [1]. The high concentrations adopted for this characterization are identical to the concentrations utilized in the ionic conductivity measurements, i.e., 0.030, 0.10, 0.30, and 1.0 eq/L, and the high:low concentration ratio is set at 5.0 (commonly used in α characterizations [22,24,25]). For example, for the high concentration of 0.30 eq/L, the low concentration would be 0.060 eq/L. Before characterization at each concentration pair, the membrane samples were immersed in an equilibration bath of the high concentration solution for 24 h, with the bath solution replaced after 12 h.

The apparent permselectivity can be defined in terms of electromigration transport numbers, t, by [1].

$$\alpha = \frac{t_{ct}^m - t_{ct}^s}{t_{co}^s} \tag{3}$$

where subscripts ct and co refer to counterion and co-ion, respectively, and superscripts m and s represent membrane phase and solution phase, respectively. For solutions containing a single electrolyte and assuming the electromigration transport numbers to be constant across the membrane thickness [23], the membrane potential, V_m, is related to t by [2].

$$V_m = -\frac{t_{ct}^m}{z_{ct}}\frac{RT}{F}\ln\frac{a_{ct}^{LC}}{a_{ct}^{HC}} - \frac{t_{co}^m}{z_{co}}\frac{RT}{F}\ln\frac{a_{co}^{LC}}{a_{co}^{HC}} \tag{4}$$

where R is the gas constant, F is the Faraday constant, T is absolute

temperature, z is ion valence, a is ion activity, and superscripts LC and HC denote low and high concentrations, respectively. Since $t_{ct}^{m} + t_{co}^{m} = 1$ and further assuming $a_{ct}^{LC}/a_{ct}^{HC} = a_{co}^{LC}/a_{co}^{HC} = a^{LC}/a^{HC}$ [2], Eq. (4) can be simplified to

$$V_m = \left(\frac{t_{ct}^{m}}{z_{ct}} + \frac{1 - t_{ct}^{m}}{z_{co}}\right) \frac{RT}{F} \ln \frac{a^{HC}}{a^{LC}} \tag{5}$$

where the activity, a, could be expressed as the product of molar concentration, c, and mean activity coefficient, $\gamma_{\pm}$, i.e., $a = \gamma_{\pm} c$. If the IEM is perfectly permselective, only counterions can permeate across the membrane, i.e., $t_{ct}^{m} = 1$; then the theoretical potential in the ideal case, V_{theo} (or, equivalently, the Nernst potential), is [1,2,26]

$$V_{theo} = \frac{RT}{z_{ct}F} \ln \frac{a^{HC}}{a^{LC}} \tag{6}$$

The number of cations and anions each electrolyte dissociates into are denoted by ν_+ and ν_-, respectively. For a ν_+:ν_- electrolyte, the expression of t_{ct}^{m} can be obtained by substituting Eq. (6) into Eq. (5) together with $z_{ct}\nu_{ct} + z_{co}\nu_{co} = 0$:

$$t_{ct}^{m} = \frac{\frac{\nu_{ct} V_m}{V_{theo}} + \nu_{co}}{\nu_{ct} + \nu_{co}} \tag{7}$$

Eq. (7) is further substituted into Eq. (3) to yield the final expression of α for a ν_+:ν_- electrolyte:

$$\alpha = \frac{1}{(\nu_{ct} + \nu_{co}) t_{co}^{s}} \left[\frac{\nu_{ct} V_m}{V_{theo}} + \nu_{co} - (\nu_{ct} + \nu_{co}) t_{ct}^{s}\right] \tag{8}$$

The equations of apparent permselectivity for various types of electrolytes in contact with CEM and AEM can be obtained by substituting the values of ν_+ and ν_- into Eq. (8). The resultant equations are summarized in Table 1 and are consistent with permselectivity expressions in literature [1,23,26].

The potential difference across the membrane, V_m, was measured using the technique described in previous studies [20,23,26] and briefly described here. Membrane coupons with an active area of 3.14 cm^2 were installed in a two-chamber cell (60 mL for each chamber), which contained high and low concentration solutions. The open-circuit potentials were measured by two Ag/AgCl reference electrodes (Single-Junction Standard Model, Fisher Scientific, Pittsburgh, PA) connected to the electrochemical workstation (Interface 1010E, Gamry Instruments, Warminster, PA). The solutions were well-mixed by stirring during the potential measurements. After the reading between the two reference electrodes had stabilized (fluctuations were within 0.1 mV over 5 min) [26–28], the potential was averaged over 15 min to give the steady state measurement. Offset potentials between the reference electrodes were recorded in the high concentration solution with the same stabilization criterion. Junction potential differences between the two reference electrodes across high and low concentration solutions were estimated using the activity-corrected form of the Henderson equation [26].

Table 1
Summary of apparent permselectivity equations for different types of electrolytes.

ν_+:ν_-	CEM	AEM
1:1 (e.g., NaCl)	$\alpha = \frac{\frac{V_m}{V_{theo}} + 1 - 2t_{ct}^{s}}{2t_{co}^{s}}$	$\alpha = \frac{\frac{V_m}{V_{theo}} + 1 - 2t_{ct}^{s}}{2t_{co}^{s}}$
1:2 (e.g., $CaCl_2$)	$\alpha = \frac{\frac{V_m}{V_{theo}} + 2 - 3t_{ct}^{s}}{3t_{co}^{s}}$	$\alpha = \frac{\frac{2V_m}{V_{theo}} + 1 - 3t_{ct}^{s}}{3t_{co}^{s}}$
1:3 (e.g., $AlCl_3$)	$\alpha = \frac{\frac{V_m}{V_{theo}} + 3 - 4t_{ct}^{s}}{4t_{co}^{s}}$	$\alpha = \frac{\frac{3V_m}{V_{theo}} + 1 - 4t_{ct}^{s}}{4t_{co}^{s}}$
2:1 (e.g., Na_2SO_4)	$\alpha = \frac{\frac{2V_m}{V_{theo}} + 1 - 3t_{ct}^{s}}{3t_{co}^{s}}$	$\alpha = \frac{\frac{V_m}{V_{theo}} + 2 - 3t_{ct}^{s}}{3t_{co}^{s}}$

Subtracting the offset potential and junction potential difference from the steady state measurement yields the membrane potential, V_m [26].

Solution phase transport numbers were determined using [29].

$$t_i^{s} = \frac{u_i}{u_{ct} + u_{co}} \tag{9}$$

where u is ion electrical mobility obtained from Ref. [12]. Using t_{ct}^{s} and t_{co}^{s} calculated with Eq. (9), the experimentally characterized V_m, and the Nernst potential computed with mean activity coefficients estimated by the Pitzer model [30,31], α can be determined through Eq. (8). Permselectivity values of at least duplicate measurements are reported for each condition tested on the same membrane coupon.

3. Results and discussion

3.1. Influence of counterion on conductivity

3.1.1. Diffusion boundary layer resistance is dominant at low electrolyte concentrations

A high ionic conductivity or, equivalently, low ionic resistance is crucial for the performance of IEM-based processes [4]. Fig. 1 shows the effective ionic conductivity, κ, of the CEM (Fig. 1A and B) and AEM (Fig. 1C and D) as a function of electrolyte concentration, c, for different counterions with co-ions fixed (Cl^- and SO_4^{2-} for CEM; Na^+ and Mg^{2+} for AEM). Note that both axes of the plots are on logarithmic scales. The results show that κ is dependent on the concentration of the external electrolyte solution. With increasing c, the conductivities first increase relatively sharply and then gradually level off (correspondingly, ASRs steeply decline and subsequently plateau). This trend is observed across all electrolyte solutions for both CEM and AEM, and, is consistent with results reported in previous studies [9,13,18,32].

The diminished κ at low concentrations is mainly due to the mass transfer resistance contribution from the diffusion boundary layer (DBL) [11,32,33]. Because of the difference in transport numbers between the aqueous solution and IEM, concentration polarization is established at the solution-membrane interfaces during ion transport, which produces a depletion of ions on one side of the IEM and ion enrichment on the other side [33–35]. Particularly for the depleted side, the lowered ion concentration leads to an elevated ionic resistance in the DBL [29,34]. The resistance characterization measures the overall resistance of the IEM and the DBLs. Therefore, the measured ASRs are the total resistances in series [1,11], and the resulting effective conductivity, κ, contains contributions of the IEM and DBLs. At low c, the resistance of the ion-depleted DBL is typically much higher than IEM resistance and, hence, dominates the effective ASR [11,18]. With increasing c, resistance of the ion-depleted DBL rapidly declines [11,18], while the IEM resistance remains almost constant [9]. Note that the practically constant IEM resistance is valid for the solution concentration range investigated in this study, which are lower than the membrane fixed charge concentrations [9]. Therefore, the DBL contribution to net resistance is lessened and the membrane resistance eventually becomes dominant with rising c. As a result, the overall ionic conductivities initially increase with higher electrolyte concentrations (κ limited by DBL) and then progressively level off at higher c (measured κ is approximately ionic conductivity of solely the IEM). This influence of DBL has been reported for NaCl solutions [18,32,34] and was quantified using electrochemical impedance spectroscopy and other techniques [11,18,35]. This study further elucidates the role of DBL resistance by extending to a broader range of various electrolytes.

The effective conductivities, i.e., the overall contributions from DBL and IEM, of both cation and anion exchange membranes in different electrolyte solutions tend to converge at the lower concentrations investigated. More specifically, κ approaches ≈0.05–0.1 S/m for both CEM and AEM at the lowest c of 0.030 eq/L in almost all electrolyte solutions, as shown in Fig. 1 and Tables 2 and 3. Similar observations

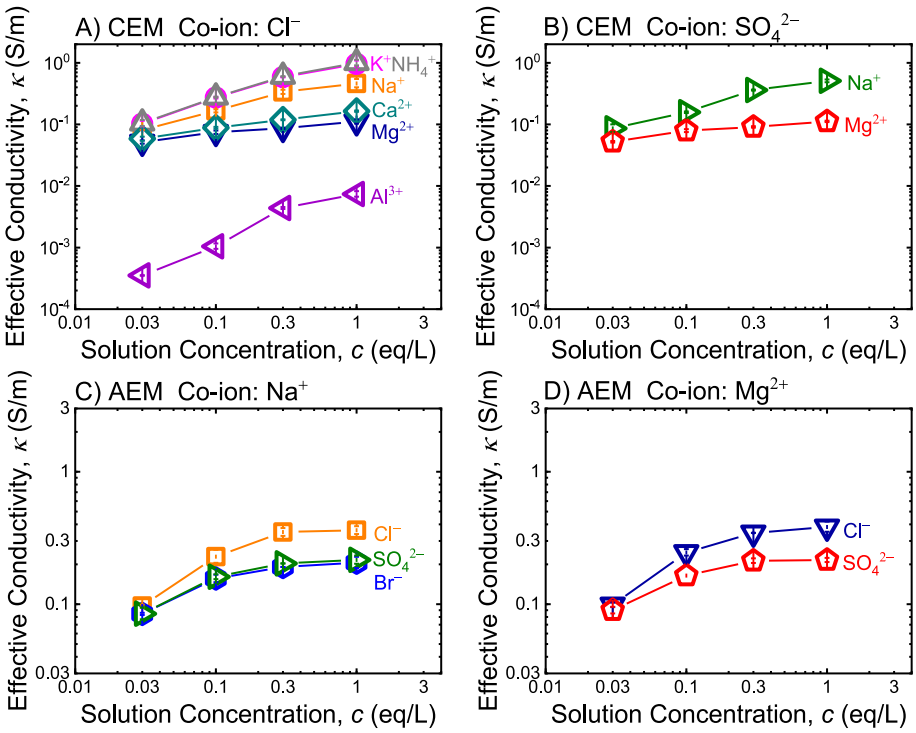

Fig. 1. Effective ionic conductivity, κ, as a function of electrolyte concentration, c, for CEM in solutions with different counterions and co-ion as A) Cl^- and B) SO_4^{2-}, and AEM in solutions with different counterions and co-ion as C) Na^+ and D) Mg^{2+}. Data points and error bars are means and standard deviations, respectively, from at least triplicate experiments on the same membrane coupon.

Table 2
Effective conductivity, κ, of CEM in various electrolyte solutions and concentrations. Values denote means and standard deviations of at least triplicate measurements on the same membrane coupon.

Concentration (eq/L)	CEM effective conductivity, κ (S/m)				
	NaCl	KCl	NH_4Cl	$MgCl_2$	$CaCl_2$
0.030	0.081 ± 0.001	0.102 ± 0.012	0.105 ± 0.013	0.052 ± 0.003	0.058 ± 0.005
0.10	0.165 ± 0.010	0.271 ± 0.009	0.277 ± 0.005	0.074 ± 0.005	0.088 ± 0.003
0.30	0.335 ± 0.028	0.583 ± 0.001	0.602 ± 0.004	0.086 ± 0.002	0.119 ± 0.002
1.0	0.461 ± 0.086	0.958 ± 0.128	1.005 ± 0.115	0.111 ± 0.009	0.164 ± 0.004
	$AlCl_3$	**NaBr**	**Na_2SO_4**	**$MgSO_4$**	
0.030	0.00035 ± 0.00000	0.087 ± 0.015	0.086 ± 0.014	0.052 ± 0.001	
0.10	0.0010 ± 0.0001	0.172 ± 0.001	0.158 ± 0.004	0.079 ± 0.004	
0.30	0.0044 ± 0.0002	0.344 ± 0.022	0.361 ± 0.006	0.091 ± 0.002	
1.0	0.0074 ± 0.0008	0.430 ± 0.052	0.508 ± 0.027	0.112 ± 0.003	

Table 3
Effective conductivity, κ, of AEM in various electrolyte solutions and concentrations. Values denote means and standard deviations of at least triplicate measurements on the same membrane coupon.

Concentration (eq/L)	AEM effective conductivity, κ (S/m)				
	NaCl	KCl	NH_4Cl	$MgCl_2$	$CaCl_2$
0.030	0.097 ± 0.002	0.096 ± 0.012	0.104 ± 0.006	0.099 ± 0.004	0.103 ± 0.000
0.10	0.228 ± 0.029	0.234 ± 0.025	0.234 ± 0.004	0.246 ± 0.015	0.248 ± 0.022
0.30	0.350 ± 0.025	0.354 ± 0.004	0.342 ± 0.008	0.345 ± 0.000	0.379 ± 0.011
1.0	0.362 ± 0.027	0.362 ± 0.055	0.400 ± 0.015	0.383 ± 0.037	0.398 ± 0.037
	$AlCl_3$	**NaBr**	**Na_2SO_4**	**$MgSO_4$**	
0.030	0.096 ± 0.005	0.084 ± 0.002	0.085 ± 0.009	0.090 ± 0.005	
0.10	0.237 ± 0.011	0.156 ± 0.011	0.161 ± 0.007	0.164 ± 0.031	
0.30	0.346 ± 0.030	0.191 ± 0.000	0.203 ± 0.001	0.213 ± 0.009	
1.0	0.405 ± 0.052	0.206 ± 0.022	0.216 ± 0.017	0.216 ± 0.008	

were reported in previous studies for other commercial and lab-fabricated IEMs [13,15]. As DBL resistance dominates at the low concentration range, the convergence in κ indicates that the limiting factor on overall transport is the diffusion current, which is proportional to the product of the valency, $|z|$, and bulk solution diffusivity, D^s, of the ions [1,29]. $|z|D^s$ of the cations and anions examined here are within a factor of 2 (1.33×10^{-9}–2.14×10^{-9} m^2/s) [12], in general agreement with the κ range at low c.

The only exception is CEM in $AlCl_3$ solution, where $\kappa \approx 0.00035$ S/m at 0.030 eq/L is around two orders of magnitude lower than other electrolytes (Fig. 1A and Table 2). This atypical behavior of Al^{3+} has been reported in a past study and was attributed to the applied current density exceeding the limiting current density [36]. Specifically, the study suggests that the process is in the over-limiting region when $AlCl_3$ concentrations in the electrolyte solutions are low during ASR characterization (application of constant current sweeps), and posits that the high resistance can possibly be explained by deposition of $Al(OH)_3$ precipitates on the anodic surface of the CEM and electrolysis of water [36]. However, we note that the difference in κ between $AlCl_3$ and other chloride electrolytes is sizeable ($>\approx150\times$) and further investigations will likely be necessary to verify if the above-mentioned phenomena can indeed quantitatively account for the considerable disparity.

3.1.2. *Higher valency counterions exhibit lower ionic conductivity*

The influence of counterion identity on the effective conductivities can be examined by comparing κ for electrolytes with the same co-ion but different counterions (i.e., analyzing the data points within each panel of Fig. 1). In general, i) κ for counterions with the same valency

tend to group together, and ii) higher valency counterions exhibit lower conductivities, with the disparity in κ greater at higher c. For example, for CEM with Cl^- as co-ion (Fig. 1A), the sequence of conductivities follows monovalent (K^+, NH_4^+, and Na^+) > divalent (Ca^{2+} and Mg^{2+}) > trivalent (Al^{3+}). Similarly, when the co-ion of AEM is Mg^{2+} (Fig. 1D), κ with monovalent counterion (Cl^-) is greater than divalent counterion (SO_4^{2-}). The same trends are also observed in Fig. 1B and C. These observations are consistent with experimental conductivity or resistance measurements reported in literature [13,14,37,38].

For the range of solution concentrations investigated here, counterion is the main charge carrier in the IEMs, i.e., ionic current due to co-ions is negligibly small [8]. Under an applied external current, ionic conductivity of just the IEM, κ^m, is effectively proportional to the product of valency, concentration, and mobility of the counterion in the membrane phase, $\kappa^m \propto \approx |z_{ct}|c_{ct}^m u_{ct}^m$ (according to the Nernst-Planck equation, the Einstein relation, and Ohm's law) [1,7,9,29,39], where superscript m denotes membrane phase. Because $|z_{ct}|c_{ct}^m$ is practically equivalent to the membrane fixed charge density in order to preserve electroneutrality [8], the product of valency and concentration can be considered to be the same for counterions with different valencies. Therefore, membrane conductivity is primarily determined by counterion mobility within the IEM, u_{ct}^m. While counterions with higher valencies generally have larger hydrated radii and correspondingly lower mobilities (the Stokes-Einstein relation) [11,12,40], electrostatic interactions between the mobile counterions and fixed charges in the membrane matrix were found to be the primary cause for the greater reduction in u_{ct}^m for higher valency counterions [41], with $u_{ct}^m \propto u_{ct}^s \exp(-z_{ct}^2)$ (superscript s denotes solution phase) [17]. The marked decrease in u_{ct}^m of counterions of higher charge has also been reported in other studies [42–44]. Because IEM resistance dominates over the contribution from DBL at greater solution concentrations, the difference in κ is more pronounced at higher c.

However, Br^- in AEM is an exception to the above-discussed trend (Fig. 1C). According to the trend, the effective conductivities of monovalent counterions are supposed to be higher than divalent counterions, but the AEM actually exhibits slightly lower conductivity in Br^- than SO_4^{2-}. This behavior was also observed in another study [13]. Possible reasons for this deviation will be discussed in Section 3.1.3.

3.1.3. Aqueous diffusivity differentiates conductivity of counterions with same valency

For counterions with the same valency, ions with greater diffusivities, D^s, or, equivalently, electrical mobility, u^s, in the bulk phase aqueous solution show higher κ. Note that $D = uRT/|z|F$ [12,29]. Again, the difference is more pronounced at higher c, where the membrane resistance is dominant. For instance, the sequence of aqueous ion electrical mobilities for three monovalent counterions in Fig. 1A is $K^+ \approx NH_4^+ > Na^+$ (7.62×10^{-8}, 7.63×10^{-8}, and 5.19×10^{-8} $m^2V^{-1}s^{-1}$, respectively) [12], which is consistent with the conductivity ranking among these counterions. The same trend is also observed for the two divalent counterions, Ca^{2+} and Mg^{2+}, where Ca^{2+} has higher u^s than Mg^{2+} (6.17×10^{-8} and 5.49×10^{-8} $m^2V^{-1}s^{-1}$, respectively) [12] and, correspondingly, κ with Ca^{2+} counterion is greater. These findings are in agreement with conductivity and resistance measurements reported in previous studies as well [13,45]. As discussed earlier, κ^m is primarily determined by counterion mobility in the membrane, u_{ct}^m. Since $u_{ct}^m \propto u_{ct}^s$ for counterions with the same valency [17], κ trends at the higher c investigated can, therefore, be explained by the electrical mobilities of the ions in bulk phase aqueous solution.

Among the counterions investigated, Br^- is observed to not conform to the above-mentioned κ trend. u^s of Br^- is very similar to Cl^- (8.09×10^{-8} and 7.91×10^{-8} $m^2V^{-1}s^{-1}$, respectively) [12]. But contrary to expectation, AEM conductivity in Br^- is much lower than Cl^- and is even slightly below SO_4^{2-} (Fig. 1C), as pointed out in Section 3.1.2 and also reported in another study [13]. This discrepancy implies that there may be factors in addition to ion electrical mobility playing a significant role in the conductivity of AEM with Br^-. Transport across IEMs can be described by the obstruction theory [46,47], where ions migrate through a tortuous path formed by the water phase of the membrane matrix, i.e., space occupied by the polymer is inaccessible. The Mackie-Meares model relates ion electrical mobilities in hydrated IEM to bulk solution phase by $u^m = u^s[f_w/(2-f_w)]^2$, where f_w is volume fraction of water in the membrane, to account for the spatial effects [46]. Swelling degree, SD, is defined as the mass ratio of sorbed water to dry polymer and is related to f_w by $f_w = SD/(SD + \rho_w/\rho_p)$, where ρ_w and ρ_p are the densities of water and polymer, respectively [20,48,49]. SD of the AEM in Br^- and Cl^- counterions were characterized as 0.129 ± 0.010 and 0.171 ± 0.005, respectively, in NaBr and NaCl electrolyte solutions using the gravimetric method [2,20]. The 24.6% lower SD with Br^- corresponds to a 21.2% reduction in membrane water volume fraction, f_w. Therefore, according to the Mackie-Meares model, the spatial effects lower the ionic conductivity of Br^- by 39.0%, relative to Cl^-, explaining the experimentally observed difference of 43.1% in Fig. 1C.

3.2. Conductivity is insensitive to co-ion identity

The influence of co-ion on the effective ionic conductivities can be investigated by examining κ of the membranes in electrolyte solutions with different co-ions but the same counterion. κ as a function of solution concentration, c, for counterions of Na^+ and Mg^{2+} for CEM and Cl^- and SO_4^{2-} for AEM are shown in Fig. 2A and B, respectively. Note that both axes of the plots are on logarithmic scales. For the same counterion,

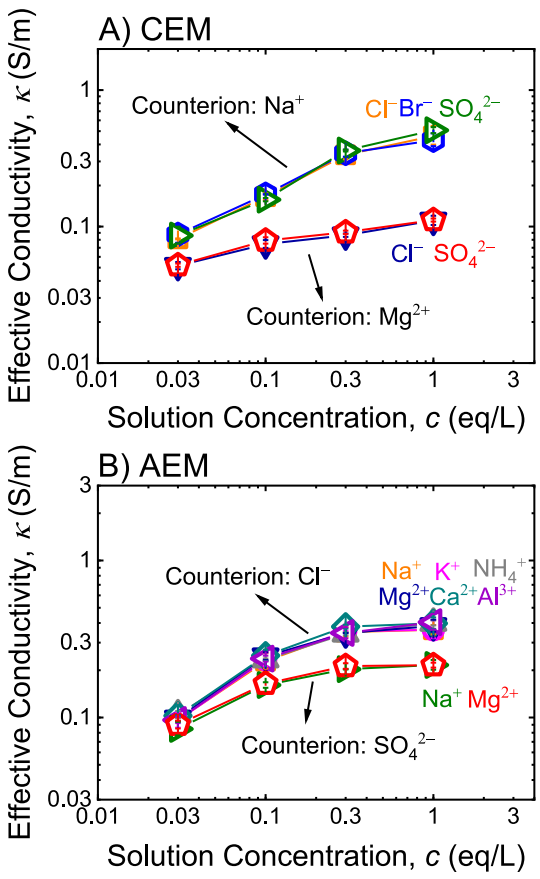

Fig. 2. Effective ionic conductivity, κ, as a function of electrolyte concentration, c, for A) CEM in solutions with different co-ions and counterion as Na^+ and Mg^{2+}, and B) AEM in solutions with different co-ions and counterion as Cl^- and SO_4^{2-}. Data points and error bars are means and standard deviations, respectively, from at least triplicate experiments on the same membrane coupon.

κ of different co-ions are effectively equal across the concentration range analyzed. Importantly, the effective ionic conductivities are practically identical i) at both low and high concentrations, where DBL and membrane resistances, respectively, are dominant (discussed earlier in Section 3.1.1); ii) for different co-ion valences (i.e., κ of mono-, di-, and trivalent co-ions are alike); and iii) for different co-ions with dissimilar electrical mobilities (e.g., NH_4^+ and Na^+ have u^s of 7.63×10^{-8} and 5.19×10^{-8} $m^2V^{-1}s^{-1}$, respectively, but undistinguishable κ). This indicates that κ is insensitive to the co-ion identity, in agreement with membrane resistances and conductivities observed in previous studies [13,38]. The insignificance of co-ions in membrane phase charge transfer is consistent with the charge exclusion effect of IEMs, which results in orders of magnitude lower concentration of co-ions than counterions within the IEMs [1,8,9]. The result here further confirms that the co-ion also plays a minor role in the resistance of DBL layer [39,50,51]. Therefore, charge transfer in both IEM and DBL is governed by counterions and the role of co-ions is insignificant.

3.3. Influence of counterion on permselectivity

3.3.1. Permselectivity is lowered at higher concentrations due to weakened charge exclusion

Permselectivity is a measure of the ability of the membrane to selectively allow for counterion transport over co-ions and is also an important parameter, along with ionic conductivity, for IEM performance; a high permselectivity is always desired in IEM-based separations [1]. Fig. 3 displays the apparent permselectivity, α, of CEM (Fig. 3A and B) and AEM (Fig. 3C and D) as a function of solution concentration, c, for various counterions but same co-ion of Cl^- or SO_4^{2-} for CEM and Na^+ or Mg^{2+} for AEM. Note that the horizontal axes are on logarithmic scales and vertical axes are on linear scales for all plots. The same data is summarized in Tables 4 and 5. Some experimentally determined apparent permselectivities values are larger than unity. This is due to experimental artifacts inherent to the α characterization method and will be further discussed in Section 3.3.2. The results indicate that α depends on the external solution concentration, with apparent permselectivities declining at an increasing rate with greater c. This deteriorating trend of apparent permselectivity is consistently observed for both CEM and AEM in the different electrolytes investigated and is in good agreement with findings of past studies [8,11,16].

Table 4
Apparent permselectivity, α, of CEM in various electrolyte solutions and concentrations. Values denote means and standard deviations of at least duplicate measurements on the same membrane coupon.

Concentration (eq/L)	CEM apparent permselectivity, α (−)				
	NaCl	KCl	NH_4Cl	$MgCl_2$	$CaCl_2$
0.030	0.988 ± 0.012	0.982 ± 0.010	0.987 ± 0.010	0.943 ± 0.008	0.945 ± 0.003
0.10	0.989 ± 0.002	0.977 ± 0.008	0.978 ± 0.006	0.933 ± 0.003	0.930 ± 0.010
0.30	0.975 ± 0.008	0.969 ± 0.005	0.962 ± 0.003	0.919 ± 0.011	0.920 ± 0.029
1.0	0.930 ± 0.027	0.910 ± 0.008	0.917 ± 0.004	0.865 ± 0.001	0.860 ± 0.008

	$AlCl_3$	NaBr	Na_2SO_4	$MgSO_4$
0.030	0.873 ± 0.016	0.983 ± 0.017	1.03 ± 0.01	0.986 ± 0.037
0.10	0.850 ± 0.010	0.982 ± 0.018	1.03 ± 0.02	0.984 ± 0.003
0.30	0.762 ± 0.006	0.971 ± 0.003	0.988 ± 0.009	0.968 ± 0.004
1.0	0.615 ± 0.017	0.934 ± 0.001	0.969 ± 0.004	0.941 ± 0.004

The lower α reflects increased transport of co-ions across the IEM, which is caused by the weakened charge exclusion at higher solution concentrations [1,7,12]. Exclusion of co-ions from the IEM is governed by the Donnan potential, the electrical potential difference at the membrane-solution interface: the sign convention of the Donnan potential is such that co-ions are repelled from the IEM (and counterions are attracted into the membrane) and the magnitude determines the extent of repulsion [1,12,52,53]. The Donnan potential is inversely proportional to the external solution concentration [1,7,54]. Thus, as c increases, the Donnan potential is diminished and the ability of IEM to

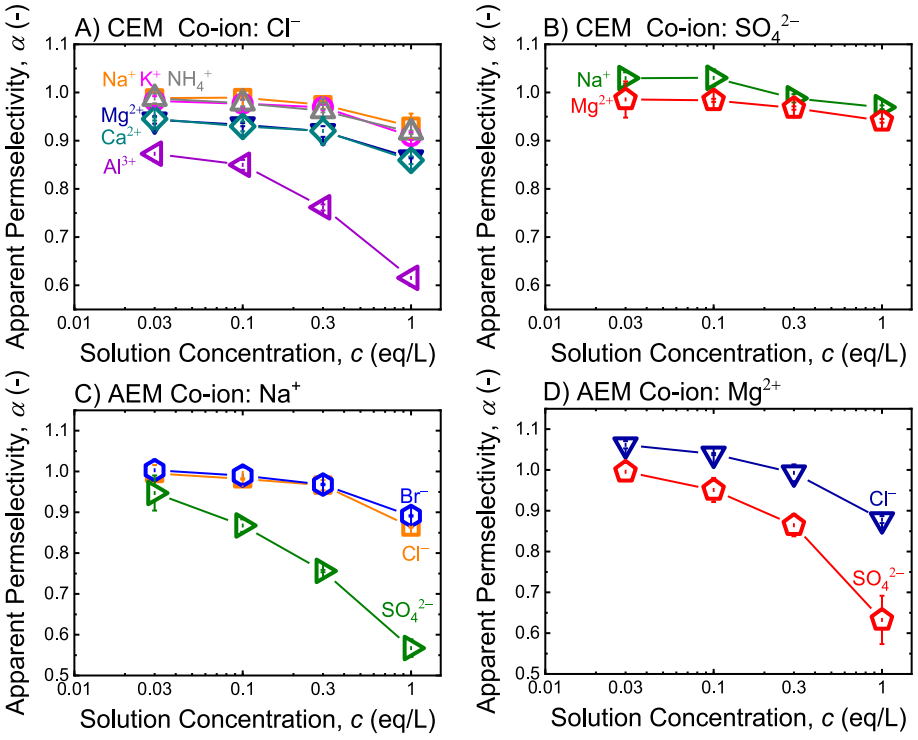

Fig. 3. Apparent permselectivity, α, as a function of electrolyte concentration, c, for CEM in solutions with different counterions and co-ion as A) Cl^- and B) SO_4^{2-}, and AEM in solutions with different counterions and co-ion as C) Na^+ and D) Mg^{2+}. Data points and error bars are means and standard deviations, respectively, from at least duplicate experiments on the same membrane coupon.

Table 5
Apparent permselectivity, α, of AEM in various electrolyte solutions and concentrations. Values denote means and standard deviations of at least duplicate measurements on the same membrane coupon.

Concentration (eq/L)	AEM apparent permselectivity, α (−)				
	NaCl	KCl	NH_4Cl	$MgCl_2$	$CaCl_2$
0.030	0.995 ± 0.021	1.00 ± 0.02	0.997 ± 0.021	1.06 ± 0.01	1.05 ± 0.00
0.10	0.982 ± 0.002	0.995 ± 0.003	0.993 ± 0.009	1.04 ± 0.00	1.04 ± 0.01
0.30	0.967 ± 0.012	0.984 ± 0.003	0.989 ± 0.011	0.993 ± 0.021	0.996 ± 0.009
1.0	0.864 ± 0.002	0.870 ± 0.008	0.869 ± 0.012	0.878 ± 0.008	0.884 ± 0.006

	$AlCl_3$	NaBr	Na_2SO_4	$MgSO_4$
0.030	1.11 ± 0.01	1.00 ± 0.03	0.947 ± 0.043	0.996 ± 0.022
0.10	1.08 ± 0.02	0.990 ± 0.020	0.868 ± 0.015	0.951 ± 0.029
0.30	1.04 ± 0.01	0.968 ± 0.002	0.756 ± 0.003	0.865 ± 0.027
1.0	0.897 ± 0.018	0.891 ± 0.002	0.567 ± 0.021	0.633 ± 0.059

exclude co-ions is suppressed [55–57], resulting in the progressive compromise of permselectivity. The effect of external solution concentration on α has been characterized in NaCl [11,14,16]. The present study widens the range of electrolytes and quantifies the influence of c on apparent permselectivity trends across different counter- and co-ion pairs.

For the well-studied NaCl, the decline in α accelerates as c increases. For instance, the CEM apparent permselectivity remains at around 0.99 when the NaCl concentration increases from 0.030 to 0.10 eq/L, but drops from 0.975 to 0.930 as c further rises from 0.30 to 1.0 eq/L (Fig. 3A and Table 4). A similar α trend is observed for AEM in NaCl. In the lower concentration range, i.e., $c < 0.10$ eq/L in Fig. 3A and C, membrane concentration of the co-ion is orders of magnitude lower than the counterion [8,54,58] and, hence, α is only slightly lowered even though the relative increase in membrane co-ion concentration is substantial due to the elevated c [8]. As the external solution concentration approaches the membrane fixed charge density (2.01 and 1.87 eq/L for the CEM and AEM in this study, respectively), the membrane concentration of co-ion gradually becomes comparable and nonnegligible relative to counterion. The charge exclusion ability of the IEMs is eventually overwhelmed when NaCl solution concentrations reach around the level of membrane fixed charge density [8,59,60]. However, α trends significantly dissimilar from NaCl are observed for some of the other electrolytes, e.g., apparent permselectivities of CEM in $AlCl_3$ and AEM in Na_2SO_4 are appreciably compromised even at solution concentrations well below the membrane fixed charge density. Possible factors contributing to such divergences are discussed next.

3.3.2. Higher valency counterions experience lower permselectivity

The impact of counterion identity on the apparent permselectivity is investigated by comparing α for electrolytes with different counterions but the same co-ion (i.e., examining the data points within each panel of Fig. 3). Trends similar to the analysis of conductivity in Section 3.1.2 were observed: i) α for counterions with same valency tend to gather into groups and ii) higher valency counterions show lower apparent permselectivity, with the difference generally more prominent in the high c range. For instance, when the co-ion is maintained as Cl^- (Fig. 3A), the order of α for CEM follows monovalent (K^+, NH_4^+, and Na^+) > divalent (Ca^{2+} and Mg^{2+}) > trivalent (Al^{3+}). Likewise, AEM exhibits greater α for monovalent counterions (Cl^- and Br^-) than the divalent counterion of SO_4^{2-}, when the co-ion is Na^+ (Fig. 3C). These features are consistent with experimental results reported in previous studies [11,14,15].

As discussed earlier, the exclusion of co-ions is governed by the Donnan potential. The Donnan potential is inversely proportional to the counterion valency [1,55,57]. Thus, higher counterion valencies will reduce the Donnan potential, giving rise to greater co-ion concentrations in the membrane matrix and eventually lowering the permselectivity [57,60,61]. Additionally, affinity between counterions and fixed charge groups can produce a screening effect that reduces the effective fixed charge density in the membrane, thus weakening the ability of IEMs to exclude co-ions [11,23]. This affinity and, hence, screening effect are generally stronger for higher valency counterions [40,62] and may also contribute to the lessened α with greater z_{ct}. The diminished co-ion exclusion by IEMs with increasing counterion valency has been found in several ion sorption studies [55,57,63].

At low concentrations, a few αs in Fig. 3 are slightly larger than unity. For example, at c of 0.030 eq/L, apparent permselectivities of CEM in Na_2SO_4 (Fig. 3B and Table 4) and AEM in $MgCl_2$ (Fig. 3D and Table 5) are experimentally determined to be 1.03 and 1.06, respectively. In principle, however, IEM permselectivity should not exceed 1, as permselectivity of 1 already signifies perfect selectivity for counterions over co-ions [1,26]. Thus, permselectivities >1 are physically not meaningful. The abnormal values can be explained by the method employed to determine *apparent* permselectivity α. As presented in Eq. (8) and Table 1, the apparent permselectivity is calculated using the ratio of the experimentally measured membrane potential to the theoretical potential, i.e., V_m/V_{theo}. However, V_m and V_{theo} can be very close at low c, such that even a small variation in the measured V_m (e.g., <1 mV) yields $V_m > V_{theo}$ and, subsequently, an apparent permselectivity surpassing unity. One primary contributor to this variation in the measured V_m is the different junction potential at the tips of reference electrodes from different compositions and concentrations between the electrode filling solution and the external test solution [26,29]. Although correcting for the activity in the Henderson equation can minimize this inaccuracy, the equation itself is based on simplifying assumptions and, hence, uncertainties cannot be completely eliminated [26]. In the present study, a discrepancy of ≈1 mV between experimental measurements and Henderson equation calculations for the junction potential difference between two reference electrodes is large enough to have some V_m slightly exceed V_{theo}, thus causing a few αs to be greater than unity; such margins in V_m have been reported in a past study [26]. Another possible factor is small but unavoidable experimental variations arising from disassembling and reassembling of the test cell between replicate measurements. While such variations can be minimized with careful techniques, they cannot be entirely eradicated and are often on the order of 1 mV [28]. Both these factors could be responsible for some α apparent permselectivities being larger than unity. Regardless of the effects of inherent limitations in the experimental characterization protocol on the absolute value of α, the qualitative trends still hold, namely, permselectivities for counterions with same valency group together and higher valency counterions lower the IEM permselectivities.

3.3.3. Specific interactions between counterions and fixed charge groups can affect IEM permselectivity

As discussed in the preceding section, the apparent permselectivities with different counterions of the same valency are very similar, as the Donnan potential is affected by the same z_{ct}. However, small but significant disparities between α are still observed, e.g., α for CEM in Na^+ is slightly higher than K^+ and NH_4^+ (Fig. 3A). The specific binding affinity between counterions and fixed charge groups could possibly explain some of these discrepancies: counterions that have greater affinity with the fixed moieties will better screen the electric field of the charged functional groups. This lowers the effective fixed charge concentration in the membrane and weakens the exclusion of like-charged co-ions, eventually leading to compromised permselectivity [23,27]. Relative to K^+ and NH_4^+, Na^+ is reported to have marginally weaker affinity with sulfonate functional group [62], which is the fixed charge moiety of the CEM used in this study. On the other hand, K^+ and NH_4^+ share very similar affinities with sulfonate [12,62]. Therefore, K^+ and NH_4^+ experience practically identical α trends, and both are slightly lower than Na^+, as is presented in Fig. 3A. However, the specific interactions

between counterions and fixed charge groups do not explain some of the other differences in α of the same valencies. In the case of the two divalent counterions in Fig. 3A, although Ca^{2+} exhibits slightly greater affinity with sulfonate groups than Mg^{2+} [62], there is no noticeable difference in α between them [37]. Additionally, Br^- is supposed to have slightly stronger affinity with the quaternary amine groups in AEM than Cl^- (according to the Hofmeister series and the Collins rule [12]), but the AEM displays somewhat higher permselectivity in Br^- than Cl^- (Fig. 3C) [64]. The inadequacy of the specific interactions between counterions and fixed charge groups to fully explain all observations implies that other factors, such as counterion size, polarizability, and interactions with co-ions, may play a role as well [27]. But overall, these effects are relatively minor compared to the influence of counterion valency. In other words, counterion valency is the primary factor governing IEM permselectivity.

3.4. Influence of co-ion on permselectivity

3.4.1. Membranes have greater permselectivity for higher valency co-ions

The influence of co-ion on apparent permselectivities is analyzed through the comparison between electrolyte solutions of different co-ions but identical counterion. Fig. 4 depicts α as a function of solution concentration, c, with various co-ions and the same counterion of Na^+ or Mg^{2+} for CEM (Fig. 4A and B, respectively) and Cl^- or SO_4^{2-} for AEM (Fig. 4C and D, respectively). Note that in all plots the horizontal axes are on a logarithmic scale and the vertical axes are on a linear scale. The experimental artefact of $\alpha > 1$ has been discussed earlier in Section 3.3.2.

Overall, i) α for co-ions with the same valency tend to group together and ii) higher valency co-ions exhibit greater apparent permselectivities. As an example, CEM shows greater α for the divalent co-ion of SO_4^{2-} than monovalent co-ions of Cl^- and Br^-, when counterion is Na^+ (Fig. 4A). Similarly, for AEM with Cl^- as counterion (Fig. 4C), the order of apparent permselectivity follows trivalent (Al^{3+}) > divalent (Ca^{2+} and Mg^{2+}) > monovalent (K^+, NH_4^+, and Na^+). The same trends are observed in Fig. 4B and D, and are in qualitative agreement with previous studies on IEM transport numbers [38,61]. The greater α for electrolytes with higher co-ion valencies is readily explained by the charge exclusion principle at Donnan equilibrium: higher valency co-ions experience greater repulsion, resulting in lower co-ion concentrations in the membrane matrix [1,53].

3.4.2. Specific co-ion effects can affect IEM permselectivity

Although the IEMs have very similar α values for different co-ions with the same valency, there are still small variations. E.g., CEM has slightly greater α in Cl^- than Br^- (for counterion of Na^+, Fig. 4A) and AEM has marginally lower apparent permselectivity for Na^+ than K^+ and NH_4^+ (with the counterion of Cl^-, Fig. 4C). These deviations in α for co-ions of the same valency has been reported in previous studies [23,64,65] and can generally be ascribed to co-ion properties of polarizability, charge density, and hydration enthalpy. Specifically, co-ions with lower polarizabilities, higher charge densities, and lower hydration enthalpies produce higher IEM permselectivities.

Co-ions with greater polarizabilities are more stable in the high dielectric environment of IEM matrices and, hence, favorably sorb into the membrane, leading to lower permselectivities [23,65]. Br^- is reported to be more polarizable compared with Cl^- [65], which can explain the lower α of CEM with Br^- in Fig. 4A. However, for other co-ions of same valency, another mechanism might be more dominant. Relative to Na^+, AEM with NH_4^+ co-ion has slightly higher apparent permselectivity (Fig. 4C), even though NH_4^+ is more polarizable [13,23]. NH_4^+ has, however, higher charge density than Na^+ because of its smaller hydrated radius [13,23] and is, thus, more excluded from the membrane matrix [23]. This eventually results in a higher α of AEM characterized in NH_4Cl than NaCl (Fig. 4C). The effects of different co-ion properties can potentially negate each other, e.g., for the two divalent co-ions in Fig. 4C, Ca^{2+} has greater charge density than Mg^{2+} but also greater polarizability [13], which can explain the almost identical α trends. A previous study postulated that co-ions with lower hydration enthalpies are excluded by the membrane to a greater extent

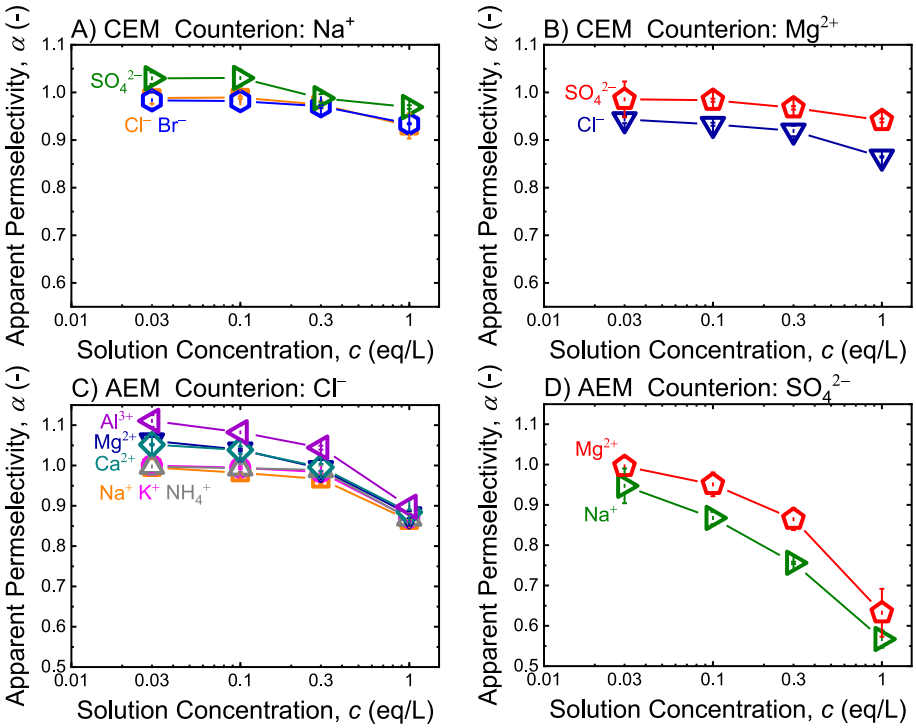

Fig. 4. Apparent permselectivity, α, as a function of electrolyte concentration, c, for CEM in solutions with different co-ions and counterion as A) Na^+ and B) Mg^{2+}, and AEM in solutions with different co-ions and counterion as C) Cl^- and D) SO_4^{2-}. Data points and error bars are means and standard deviations, respectively, from at least duplicate experiments on the same membrane coupon.

[64], thus providing a rationale for the slightly higher α in NH_4^+ than Na^+ (Fig. 4C), since NH_4^+ has comparatively lower hydration enthalpy. The study, however, did not further elaborate on the underlying principles for hydration enthalpy to influence co-ion exclusion. The above-mentioned factors can contribute to the different α observed for co-ions with same valency, but deeper understanding of the fundamental phenomena will be required to more precisely elucidate the relative importance of each effect. Crucially, these factors play a minor role in comparison to co-ion valency, i.e., valency is the principal co-ion property affecting IEM permselectivity.

3.5. Influence of counterion on the concentration-induced conductivity-permselectivity tradeoff

3.5.1. External solutions concentrations cause tradeoff between conductivity and permselectivity

As discussed in previous sections, both the effective ionic conductivity and the apparent permselectivity are influenced by the electrolyte and concentration of the external solution, c. Fig. 5 depicts α and κ with increasing c, indicated by the black arrows, for CEM (Fig. 5A, B, and C) and AEM (Fig. 5D and E). Each panel shows the κ-α trends with different counterions but the same co-ion (Cl^- or SO_4^{2-} for CEM and Na^+ or Mg^{2+} for AEM). Note that horizontal axes in Fig. 5A, B, and C are on logarithmic scales, whereas horizontal axes in Fig. 5D and E are on linear scales; vertical axes in all five plots are on linear scales. Fig. 5B displays the data of Fig. 5A but without Al^{3+} for better visualization of the other counterions (κ and α of Al^{3+} are significantly lower). As c rises, apparent permselectivity deteriorates and effective conductivity increases for all electrolytes, i.e., the external solution concentration produces a tradeoff between α and κ, as indicated by negative slopes in Fig. 5. Such tradeoff relationship has been reported in recent studies on Na^+ and Cl^- [8–10] and are extended to a wider range of ionic species here to investigate the role of counter- and co-ions on the κ-α trends.

The external solution concentration concomitantly affects the effective conductivities and apparent permselectivities (as explained in Sections 3.1.1 and 3.3.1, respectively). Specifically, raising c lowers the DBL resistance, thus enhancing the effective conductivity, particularly in the low concentration range of <0.1 eq/L. At the same time, as c increases, the Donnan potential declines and charge exclusion is weakened, resulting in the progressive diminishing of α, especially as c approaches the membrane fixed charge density. Further analysis reveals that the κ-α tradeoff relationships in Fig. 5 are influenced by the counter- and co-ion identities, and are discussed next.

3.5.2. Higher valency counterions exhibit lower conductivities and permselectivities

The effect of counterions on the tradeoff relationship can be evaluated through the comparison of κ-α profiles for different counterions but the same co-ion, i.e., each panel in Fig. 5. Generally, i) counterions with identical valency have tradeoff trends that tend to group together and ii) counterions with higher valency exhibit relatively more inferior effective conductivities and apparent permselectivities, particularly at higher

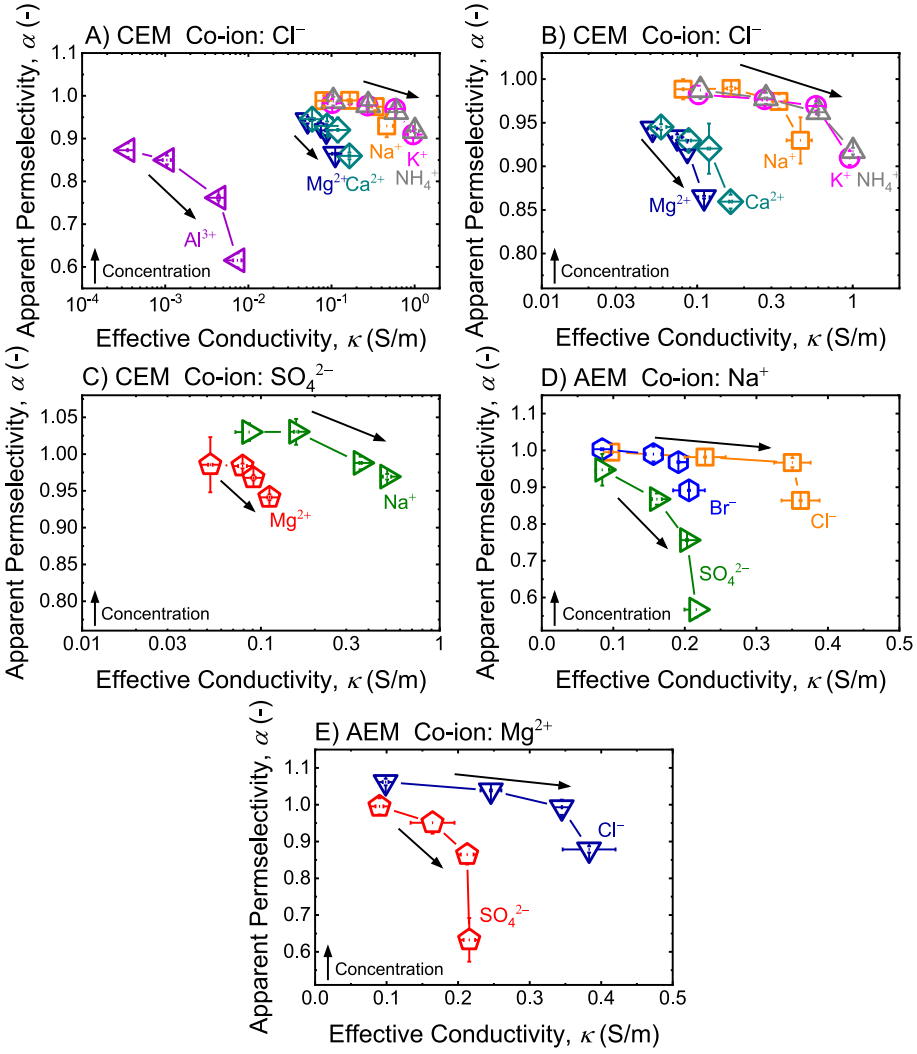

Fig. 5. Apparent permselectivity, α, and effective ionic conductivity, κ, (vertical and horizontal axes, respectively) for different electrolyte concentrations, c, of 0.030, 0.10, 0.30, and 1.0 eq/L. CEM is in solutions with different counterions and the same co-ions of A) Cl^-, B) Cl^-, but with Al^{3+} counterion data not presented, and C) SO_4^{2-}. AEM is in solutions with different counterions and the same co-ions of D) Na^+ and E) Mg^{2+}. Direction of black arrows indicates increasing c. Data points and error bars are means and standard deviations, respectively, from at least triplicate experiments for κ and duplicate experiments for α on the same membrane coupon.

solution concentrations. For example, CEM κ-α tradeoff curves with Cl^- as the co-ion shift towards the bottom-left going from monovalent (K^+, NH_4^+, and Na^+) to divalent (Ca^{2+} and Mg^{2+}) to trivalent (Al^{3+}), as depicted in Fig. 5A and B. Likewise, when Mg^{2+} is the co-ion (Fig. 5E), AEM shows lower conductivities and permselectivities for the divalent counterion of SO_4^{2-} than monovalent Cl^- at each concentration level. These trends underscore the principal importance of counterion valency on κ and α. Specifically, z_{ct} determines the electrostatic interactions between mobile counterions and membrane fixed charges, with counterions of higher valency counterions experiencing greater retardation (i.e., reduced u_{ct}^m) and, hence, lower IEM conductivity (Section 3.1.2). On the other hand, counterions of higher valencies have a larger effect on depressing the Donnan potential and screening the effective fixed charge density, thus causing lower permselectivities by diminishing the exclusion of co-ions from the membrane matrix (Section 3.3.2).

3.5.3. *Counterions with same valency show similar permselectivities but different conductivities*

Counterions of the same valency generally have small disparities in α, but significant variance in κ, i.e., the tradeoff curves are stretched/compressed along the horizontal axis about the lowest c in the permselectivity-conductivity plots of Fig. 5. The differences in κ are mainly due to the dissimilar ion electrical mobilities in aqueous solution, with counterions of greater u_{ct}^s ($\propto u_{ct}^m$) showing higher effective conductivities (Section 3.1.3). For instance, CEM conductivities in the three monovalent counterions in Fig. 5B are $K^+ \approx NH_4^+ > Na^+$, matching the order of u_{ct}^s, whereas apparent permselectivities are close among these counterions. Therefore, compressing the tradeoff curves of K^+ and NH_4^+ roughly yields the trend for Na^+. Similarly for the two divalent counterions in Fig. 5A, κ with Ca^{2+} is greater than Mg^{2+} (u_{ct}^s of $Ca^{2+} > Mg^{2+}$) but α is almost indistinguishable. Thus, stretching the tradeoff curve of Mg^{2+} gives the trend of Ca^{2+}. Counterion of Br^- in AEM is an exception (Fig. 5D): although Br^- and Cl^- have very similar u_{ct}^s, AEM shows much smaller conductivities in Br^- than Cl^-, but α are generally alike (yielding a compression from the tradeoff curve of Cl^- to Br^-). This atypical behavior can be primarily attributed to the lower water uptake of AEM in NaBr solution, which leads to more tortuous transport pathways and, hence, lower counterion mobility in the membrane matrix [46]. Some of the marginal discrepancies in α can be caused by the different binding affinity between specific counterions and fixed charge groups (as discussed in Section 3.3.3). However, the mechanism alone is not able to fully explain all observed behaviors, suggesting there might be other underlying causes. Nonetheless, the influence of counterion valency is still dominant in governing the conductivity-permselectivity tradeoff.

3.6. *Higher valency co-ions exhibit higher permselectivity but similar conductivity*

The influence of co-ions on the concentration-induced tradeoff between effective conductivity and apparent permselectivity is evaluated by comparing κ-α trends with different co-ions but the same counterion. α and κ across a range of solution concentrations, c, for CEM (Fig. 6A and B, with counterion of Na^+ and Mg^{2+}, respectively) and AEM (Fig. 6C and D, with counterion of Cl^- and SO_4^{2-}, respectively) are shown in Fig. 6. Note that both axes of all plots are on linear scales. Overall, i) κ-α profiles tend to group together for co-ions having the same valency and ii) co-ions of higher valency show similar conductivities but higher permselectivities, i.e., tradeoff curves are shifted vertically upwards. E.g., the CEM conductivity-permselectivity tradeoff curve of divalent co-ion SO_4^{2-} is higher than monovalent Cl^- and Br^- with Na^+ as the counterion (Fig. 6A) and the AEM κ-α curve of divalent co-ion Mg^{2+} is above monovalent Na^+ with counterion of SO_4^{2-} (Fig. 6D). Similar observations can be found in Fig. 6B and C. As discussed in Section 3.2, effective conductivity is not sensitive to the co-ion identity since co-ions only play a minor role in the charge transfer of both IEM and DBL. Therefore, the effect of co-ions on κ-α tradeoffs is mainly reflected in the apparent permselectivity, i.e., along the vertical axes in Fig. 6. Higher valency co-ions experience greater charge exclusion from the membrane matrix, thus resulting in larger α (Section 3.4.1) and, consequently, the tradeoff curves are shifted upwards. For co-ions of the same valency, the small disparities in apparent permselectivities can be explained by specific ion properties as detailed in Section 3.4.2. However, these effects are comparatively insignificant in relation to co-ion valency. Hence, similar behaviors in the κ-α tradeoff are observed for co-ions of the same

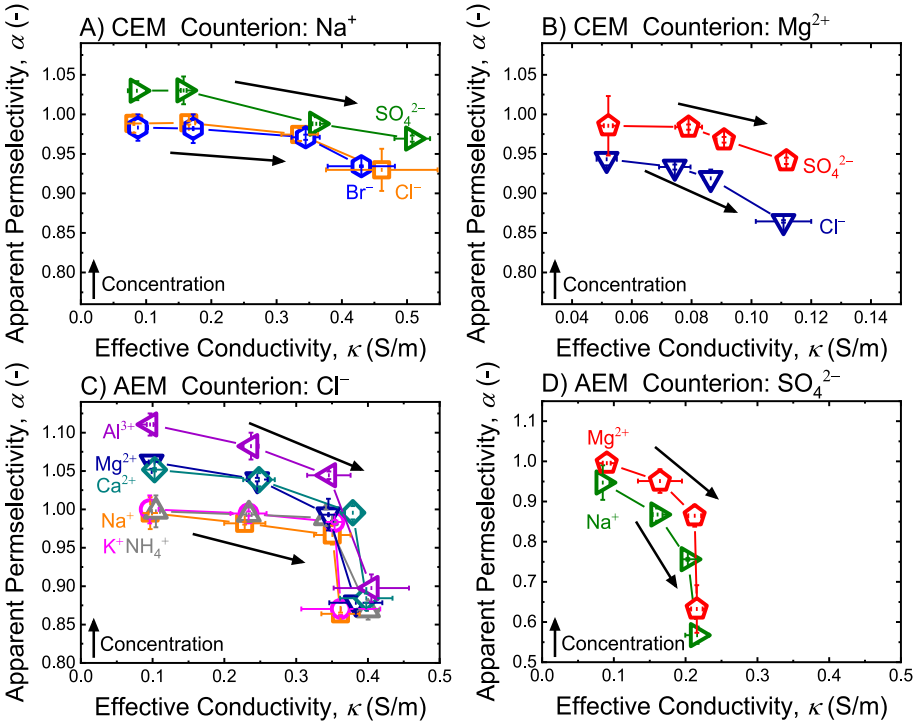

Fig. 6. Apparent permselectivity, α, and effective ionic conductivity, κ, (vertical and horizontal axes, respectively) for different electrolyte concentrations, c, of 0.030, 0.10, 0.30, and 1.0 eq/L. CEM is in solutions with different co-ions and the same counterion of A) Na^+ and B) Mg^{2+}, and AEM is in solutions with different co-ions and the same counterion of C) Cl^- and D) SO_4^{2-}. Direction of black arrows indicates increasing c. Data points and error bars are means and standard deviations, respectively, from at least triplicate experiments for κ and duplicate experiments for α on the same membrane coupon.

valency, such as CEM with Cl^- and Br^- (Fig. 6A), as well as AEM with Na^+, K^+, and NH_4^+ (Fig. 6C).

4. Implications

This study investigates the impacts of electrolytes on the concentration-induced tradeoff relationship between effective conductivity and apparent permselectivity of a cation exchange membrane and an anion exchange membrane. For the concentration range examined, the dependence of IEM effective conductivity on external solution concentration is due to the contribution of mass transfer resistance from the diffusion boundary layer. On the other hand, apparent permselectivity declines with higher external concentrations due to suppression of the Donnan potential to exclude co-ions. These concomitant effects result in a tradeoff: raising the external solution concentration enhances κ but compromises α. Such tradeoff has been reported for NaCl in past studies [8,9,66]; the present work further extends to a broader range of electrolytes to shed light on the roles of counter- and co-ion identity. The analysis shows that counterions with higher valencies lower both conductivities and permselectivities of the IEMs. For counterions of the same valency, permselectivities are largely similar but conductivities are different, which is chiefly due to disparate aqueous ion diffusivities. Co-ions are found to have insignificant influence on conductivity, but higher co-ion valencies elevate IEM permselectivities.

Ionic conductivities or, equivalently, ionic resistances, and apparent permselectivities evaluated under specific characterization conditions are often reported as constant IEM properties by membrane manufacturers and in literature [24,25]. However, κ and α are demonstrated to be dependent on concentration and electrolyte of the solution, rather than being invariant properties intrinsic to the membrane. Engineered IEM applications, such as redox flow batteries and electrodialysis of brackish groundwater, involve electrolyte solutions beyond NaCl or handle mixed electrolytes, respectively. Therefore, the solution-dependence of conductivity and permselectivity has pertinent implications for IEM-based processes and should be explicitly considered. High membrane conductivity and permselectivity are almost always desired in IEM applications, but membrane performance is inescapably constrained by the κ-α tradeoff. The low conductivities at lower solution concentrations can be alleviated by hydrodynamically depressing the diffusion boundary layers [32], but the enhancement would likely be at the expense of greater pumping energy costs to overcome the elevated parasitic pressure drops. Innovations in membrane development to attain greater conductivity and permselectivity are also actively being pursued [3,20,67]. Findings of the present study on the influence of counter- and co-ions on the tradeoff can inform the κ and α achievable, and provide guidance for the development of IEM applications. The principal factors identified in this study, such as counterion valency, counterion aqueous diffusivity, and co-ion valency, can be utilized to inform the formulation of theoretical frameworks capable of *a priori* quantitative descriptions of κ and α in different solution concentrations and compositions.

Author statement

Yuxuan Huang: Conceptualization, Methodology, Investigation, Formal analysis, Visualization, Writing - Original Draft; Hanqing Fan: Conceptualization, Methodology, Formal analysis, Writing- Reviewing and Editing; Ngai Yin Yip: Conceptualization, Supervision, Funding acquisition, Writing- Reviewing and Editing.

Declaration of competing interest

The authors declare that they have no known competing financial interests or personal relationships that could have appeared to influence the work reported in this paper.

Data availability

Data will be made available on request.

Acknowledgements

Acknowledgments are made to the anonymous reviewers for their critical reading of the manuscript and suggestions to improve the analysis and discussions.

References

[1] H. Strathmann, Ion-Exchange Membrane Separation Processes, Elsevier, 2004.
[2] T. Sata, Ion Exchange Membranes: Preparation, Characterization, Modification and Application, The Royal Society of Chemistry, Cambridge, 2004.
[3] J. Ran, L. Wu, Y. He, Z. Yang, Y. Wang, C. Jiang, L. Ge, E. Bakangura, T. Xu, Ion exchange membranes: new developments and applications, J. Membr. Sci. 522 (2017) 267–291, https://doi.org/10.1016/j.memsci.2016.09.033.
[4] T. Xu, Ion exchange membranes: state of their development and perspective, J. Membr. Sci. 263 (2005) 1–29, https://doi.org/10.1016/j.memsci.2005.05.002.
[5] H. Strathmann, Electrodialysis, a mature technology with a multitude of new applications, Desalination 264 (2010) 268–288, https://doi.org/10.1016/j.desal.2010.04.069.
[6] C. Ponce de León, A. Frías-Ferrer, J. González-García, D.A. Szánto, F.C. Walsh, Redox flow cells for energy conversion, J. Power Sources 160 (2006) 716–732, https://doi.org/10.1016/j.jpowsour.2006.02.095.
[7] H. Strathmann, A. Grabowski, G. Eigenberger, Ion-exchange membranes in the chemical process industry, Ind. Eng. Chem. Res. 52 (2013) 10364–10379, https://doi.org/10.1021/ie4002102.
[8] H. Fan, N.Y. Yip, Elucidating conductivity-permselectivity tradeoffs in electrodialysis and reverse electrodialysis by structure-property analysis of ion-exchange membranes, J. Membr. Sci. 573 (2019) 668–681, https://doi.org/10.1016/j.memsci.2018.11.045.
[9] J. Kamcev, R. Sujanani, E.-S. Jang, N. Yan, N. Moe, D.R. Paul, B.D. Freeman, Salt concentration dependence of ionic conductivity in ion exchange membranes, J. Membr. Sci. 547 (2018) 123–133, https://doi.org/10.1016/j.memsci.2017.10.024.
[10] A.H. Galama, D.A. Vermaas, J. Veerman, M. Saakes, H.H.M. Rijnaarts, J.W. Post, K. Nijmeijer, Membrane resistance: the effect of salinity gradients over a cation exchange membrane, J. Membr. Sci. 467 (2014) 279–291, https://doi.org/10.1016/j.memsci.2014.05.046.
[11] E. Fontananova, D. Messana, R.A. Tufa, I. Nicotera, V. Kosma, E. Curcio, W. van Baak, E. Drioli, G. Di Profio, Effect of solution concentration and composition on the electrochemical properties of ion exchange membranes for energy conversion, J. Power Sources 340 (2017) 282–293, https://doi.org/10.1016/j.jpowsour.2016.11.075.
[12] T. Luo, S. Abdu, M. Wessling, Selectivity of ion exchange membranes: a review, J. Membr. Sci. 555 (2018) 429–454, https://doi.org/10.1016/j.memsci.2018.03.051.
[13] S. Zhu, R.S. Kingsbury, D.F. Call, O. Coronell, Impact of solution composition on the resistance of ion exchange membranes, J. Membr. Sci. 554 (2018) 39–47, https://doi.org/10.1016/j.memsci.2018.02.050.
[14] R.K. Nagarale, G.S. Gohil, V.K. Shahi, G.S. Trivedi, R. Rangarajan, Preparation and electrochemical characterization of cation- and anion-exchange/polyaniline composite membranes, J. Colloid Interface Sci. 277 (2004) 162–171, https://doi.org/10.1016/j.jcis.2004.04.027.
[15] G. Gohil, Comparative studies on electrochemical characterization of homogeneous and heterogeneous type of ion-exchange membranes, J. Membr. Sci. 240 (2004) 211–219, https://doi.org/10.1016/j.memsci.2004.04.022.
[16] A. Zlotorowicz, R.V. Strand, O.S. Burheim, Ø. Wilhelmsen, S. Kjelstrup, The permselectivity and water transference number of ion exchange membranes in reverse electrodialysis, J. Membr. Sci. 523 (2017) 402–408, https://doi.org/10.1016/j.memsci.2016.10.003.
[17] H. Fan, Y. Huang, I.H. Billinge, S.M. Bannon, G.M. Geise, N.Y. Yip, Counterion mobility in ion-exchange membranes: spatial effect and valency-dependent electrostatic interaction, ACS EST Eng 2 (2022) 1274–1286, https://doi.org/10.1021/acsestengg.1c00457.
[18] P. Długołęcki, P. Ogonowski, S.J. Metz, M. Saakes, K. Nijmeijer, M. Wessling, On the resistances of membrane, diffusion boundary layer and double layer in ion exchange membrane transport, J. Membr. Sci. 349 (2010) 369–379, https://doi.org/10.1016/j.memsci.2009.11.069.
[19] B. Auclair, V. Nikonenko, C. Larchet, M. Métayer, L. Dammak, Correlation between transport parameters of ion-exchange membranes, J. Membr. Sci. 195 (2002) 89–102, https://doi.org/10.1016/S0376-7388(01)00556-7.
[20] H. Fan, Y. Huang, N.Y. Yip, Advancing the conductivity-permselectivity tradeoff of electrodialysis ion-exchange membranes with sulfonated CNT nanocomposites, J. Membr. Sci. 610 (2020), 118259, https://doi.org/10.1016/j.memsci.2020.118259.
[21] C. Larchet, L. Dammak, B. Auclair, S. Parchikov, V. Nikonenko, A simplified procedure for ion-exchange membrane characterisation, New J. Chem. 28 (2004) 1260–1267, https://doi.org/10.1039/B316725A.

[22] G.M. Geise, M.A. Hickner, B.E. Logan, Ionic resistance and permselectivity tradeoffs in anion exchange membranes, ACS Appl. Mater. Interfaces 5 (2013) 10294–10301, https://doi.org/10.1021/am403207w.
[23] G.M. Geise, H.J. Cassady, D.R. Paul, B.E. Logan, M.A. Hickner, Specific ion effects on membrane potential and the permselectivity of ion exchange membranes, Phys. Chem. Chem. Phys. 16 (2014) 21673–21681, https://doi.org/10.1039/c4cp03076a.
[24] P. Dlugolecki, K. Nymeijer, S. Metz, M. Wessling, Current status of ion exchange membranes for power generation from salinity gradients, J. Membr. Sci. 319 (2008) 214–222, https://doi.org/10.1016/j.memsci.2008.03.037.
[25] E. Güler, R. Elizen, D.A. Vermaas, M. Saakes, K. Nijmeijer, Performance-determining membrane properties in reverse electrodialysis, J. Membr. Sci. 446 (2013) 266–276, https://doi.org/10.1016/j.memsci.2013.06.045.
[26] R.S. Kingsbury, S. Flotron, S. Zhu, D.F. Call, O. Coronell, Junction potentials bias measurements of ion exchange membrane permselectivity, Environ. Sci. Technol. 52 (2018) 4929–4936, https://doi.org/10.1021/acs.est.7b05317.
[27] H.J. Cassady, E.C. Cimino, M. Kumar, M.A. Hickner, Specific ion effects on the permselectivity of sulfonated poly(ether sulfone) cation exchange membranes, J. Membr. Sci. 508 (2016) 146–152, https://doi.org/10.1016/j.memsci.2016.02.048.
[28] Y. Ji, G.M. Geise, The role of experimental factors in membrane permselectivity measurements, Ind. Eng. Chem. Res. 56 (2017) 7559–7566, https://doi.org/10.1021/acs.iecr.7b01512.
[29] A.J. Bard, L.R. Faulkner, Electrochemical Methods: Fundamentals and Applications, second ed., Wiley, New York, 2001.
[30] K.S. Pitzer, G. Mayorga, Thermodynamics of electrolytes. II. Activity and osmotic coefficients for strong electrolytes with one or both ions univalent, J. Phys. Chem. 77 (1973) 2300–2308, https://doi.org/10.1021/j100638a009.
[31] K.S. Pitzer, G. Mayorga, Thermodynamics of electrolytes. III. Activity and osmotic coefficients for 2–2 electrolytes, J. Solut. Chem. 3 (1974) 539–546, https://doi.org/10.1007/BF00648138.
[32] P. Długołęcki, B. Anet, S.J. Metz, K. Nijmeijer, M. Wessling, Transport limitations in ion exchange membranes at low salt concentrations, J. Membr. Sci. 346 (2010) 163–171, https://doi.org/10.1016/j.memsci.2009.09.033.
[33] J.-S. Park, J.-H. Choi, J.-J. Woo, S.-H. Moon, An electrical impedance spectroscopic (EIS) study on transport characteristics of ion-exchange membrane systems, J. Colloid Interface Sci. 300 (2006) 655–662, https://doi.org/10.1016/j.jcis.2006.04.040.
[34] B. Zhang, J.G. Hong, S. Xie, S. Xia, Y. Chen, An integrative modeling and experimental study on the ionic resistance of ion-exchange membranes, J. Membr. Sci. 524 (2017) 362–369, https://doi.org/10.1016/j.memsci.2016.11.050.
[35] J.-H. Choi, J.-S. Park, S.-H. Moon, Direct measurement of concentration distribution within the boundary layer of an ion-exchange membrane, J. Colloid Interface Sci. 251 (2002) 311–317, https://doi.org/10.1006/jcis.2002.8407.
[36] J.H. Choi, H.J. Lee, S.H. Moon, Effects of electrolytes on the transport phenomena in a cation-exchange membrane, J. Colloid Interface Sci. 238 (2001) 188–195, https://doi.org/10.1006/jcis.2001.7510.
[37] R.K. Nagarale, G.S. Gohil, V.K. Shahi, R. Rangarajan, Preparation and electrochemical characterizations of cation-exchange membranes with different functional groups, Colloids Surf. A Physicochem. Eng. Asp. 251 (2004) 133–140, https://doi.org/10.1016/j.colsurfa.2004.09.028.
[38] V.V. Sarapulova, V.D. Titorova, V.V. Nikonenko, N.D. Pismenskaya, Transport characteristics of homogeneous and heterogeneous ion-exchange membranes in sodium chloride, calcium chloride, and sodium sulfate solutions, Membr. Membr. Technol. 1 (2019) 168–182, https://doi.org/10.1134/S2517751619030041.
[39] F.G. Helfferich, Ion Exchange, Courier Corporation, 1995.
[40] H. Strathmann, 2.14 - electromembrane processes: basic aspects and applications, in: E. Drioli, L. Giorno (Eds.), Comprehensive Membrane Science and Engineering, Elsevier, Oxford, 2010, pp. 391–429, https://doi.org/10.1016/B978-0-08-093250-7.00048-7.
[41] T. Badessa, V. Shaposhnik, The electrodialysis of electrolyte solutions of multi-charged cations, J. Membr. Sci. 498 (2016) 86–93, https://doi.org/10.1016/j.memsci.2015.09.017.
[42] S. Logette, C. Eysseric, G. Pourcelly, A. Lindheimer, C. Gavach, Selective permeability of a perfluorosulphonic membrane to different valency cations. Ion-exchange isotherms and kinetic aspects, J. Membr. Sci. 144 (1998) 259–274, https://doi.org/10.1016/S0376-7388(98)00062-3.
[43] A. Goswami, A. Acharya, A.K. Pandey, Study of self-diffusion of monovalent and divalent cations in nafion-117 ion-exchange membrane, J. Phys. Chem. B 105 (2001) 9196–9201, https://doi.org/10.1021/jp010529y.
[44] H. Miyoshi, Diffusion coefficients of ions through ion excange membrane in Donnan dialysis using ions of different valence, J. Membr. Sci. 141 (1998) 101–110, https://doi.org/10.1016/S0376-7388(97)00297-4.
[45] X.T. Le, Concentration polarization and conductance of cation exchange membranes in sulfuric acid and alkaline sulfate media, J. Membr. Sci. (2012) 397–398, https://doi.org/10.1016/j.memsci.2012.01.011, 66–79.
[46] J.S. Mackie, P. Meares, E.K. Rideal, The diffusion of electrolytes in a cation-exchange resin membrane I. Theoretical, Proc. Roy. Soc. London. Ser. A. Math. Phys. Sci. 232 (1955) 498–509, https://doi.org/10.1098/rspa.1955.0234.
[47] J.S. Mackie, P. Meares, E.K. Rideal, The diffusion of electrolytes in a cation-exchange resin membrane. II. Experimental, Proc. Roy. Soc. London. Ser. A. Math. Phys. Sci. 232 (1955) 510–518, https://doi.org/10.1098/rspa.1955.0235.
[48] R.S. Kingsbury, S. Zhu, S. Flotron, O. Coronell, Microstructure determines water and salt permeation in commercial ion-exchange membranes, ACS Appl. Mater. Interfaces 10 (2018) 39745–39756, https://doi.org/10.1021/acsami.8b14494.
[49] J. Kamcev, D.R. Paul, B.D. Freeman, Ion activity coefficients in ion exchange polymers: applicability of Manning's counterion condensation theory, Macromolecules 48 (2015) 8011–8024, https://doi.org/10.1021/acs.macromol.5b01654.
[50] K.S. Spiegler, Polarization at ion exchange membrane-solution interfaces, Desalination 9 (1971) 367–385, https://doi.org/10.1016/0011-9164(71)80005-X.
[51] Y. Tanaka, Concentration polarization in ion-exchange membrane electrodialysis—the events arising in a flowing solution in a desalting cell, J. Membr. Sci. 216 (2003) 149–164, https://doi.org/10.1016/S0376-7388(03)00067-X.
[52] J. Kamcev, Ion Sorption and Transport in Ion Exchange Membranes Importance of Counter-ion Condensation, The University of Texas at Austin, 2016.
[53] Hanqing Fan, Yuxuan Huang, Ngai Yin Yip, Advancing Ion-Exchange Membranes to Ion-Selective Membranes: Principles, Status, and Opportunities, Front. Environ. Sci. Eng. 17 (2) (2022) 25, https://doi.org/10.1007/s11783-023-1625-0.
[54] J.W.P.A.H. Galama, H.V.M. Hamelers, V.V. Nikonenko, P.M. Biesheuvel, On the origin of the membrane potential arising across densely charged ion exchange membranes, how well does the Teorell-Meyer-sievers theory work, J. Membr. Sci. Res. 2 (2016) 128–140.
[55] M. Galizia, F.M. Benedetti, D.R. Paul, B.D. Freeman, Monovalent and divalent ion sorption in a cation exchange membrane based on cross-linked poly (p-styrene sulfonate-co-divinylbenzene), J. Membr. Sci. 535 (2017) 132–142, https://doi.org/10.1016/j.memsci.2017.04.007.
[56] Q. Wang, G.Q. Chen, S.E. Kentish, Sorption and diffusion of organic acid ions in anion exchange membranes: acetate and lactate ions as a case study, J. Membr. Sci. 614 (2020), 118534, https://doi.org/10.1016/j.memsci.2020.118534.
[57] G.Q. Chen, K. Wei, A. Hassanvand, B.D. Freeman, S.E. Kentish, Single and binary ion sorption equilibria of monovalent and divalent ions in commercial ion exchange membranes, Water Res. 175 (2020), 115681, https://doi.org/10.1016/j.watres.2020.115681.
[58] J. Kamcev, D.R. Paul, B.D. Freeman, Effect of fixed charge group concentration on equilibrium ion sorption in ion exchange membranes, J. Mater. Chem. A 5 (2017) 4638–4650, https://doi.org/10.1039/c6ta07954g.
[59] A. Daniilidis, D.A. Vermaas, R. Herber, K. Nijmeijer, Experimentally obtainable energy from mixing river water, seawater or brines with reverse electrodialysis, Renew. Energy 64 (2014) 123–131, https://doi.org/10.1016/j.renene.2013.11.001.
[60] M. Galizia, G.S. Manning, D.R. Paul, B.D. Freeman, Ion partitioning between brines and ion exchange polymers, Polymer 165 (2019) 91–100, https://doi.org/10.1016/j.polymer.2019.01.026.
[61] H. Luo, W.-A.S. Agata, G.M. Geise, Connecting the ion separation factor to the sorption and diffusion selectivity of ion exchange membranes, Ind. Eng. Chem. Res. 59 (2020) 14189–14206, https://doi.org/10.1021/acs.iecr.0c02457.
[62] G.M. Geise, D.R. Paul, B.D. Freeman, Fundamental water and salt transport properties of polymeric materials, Prog. Polym. Sci. 39 (2014) 1–42, https://doi.org/10.1016/j.progpolymsci.2013.07.001.
[63] J. Kamcev, D.R. Paul, G.S. Manning, B.D. Freeman, Predicting salt permeability coefficients in highly swollen, highly charged ion exchange membranes, ACS Appl. Mater. Interfaces 9 (2017) 4044–4056, https://doi.org/10.1021/acsami.6b14902.
[64] Y. Ji, H. Luo, G.M. Geise, Effects of fixed charge group physicochemistry on anion exchange membrane permselectivity and ion transport, Phys. Chem. Chem. Phys. 22 (2020) 7283–7293, https://doi.org/10.1039/d0cp00018c.
[65] Y. Ji, H. Luo, G.M. Geise, Specific co-ion sorption and diffusion properties influence membrane permselectivity, J. Membr. Sci. 563 (2018) 492–504, https://doi.org/10.1016/j.memsci.2018.06.010.
[66] R.S. Kingsbury, O. Coronell, Modeling and validation of concentration dependence of ion exchange membrane permselectivity: significance of convection and Manning's counter-ion condensation theory, J. Membr. Sci. (2020), 118411, https://doi.org/10.1016/j.memsci.2020.118411.
[67] V.I. Zabolotskii, S.A. Loza, M.V. Sharafan, Physicochemical properties of profiled heterogeneous ion-exchange membranes, Russ. J. Electrochem. 41 (2005) 1053–1060, https://doi.org/10.1007/s11175-005-0180-2.